論 文 の 内 容 の 要 旨

論文題目　Analytical studies on reaction mechanisms of hard carbon electrode as a sodium-ion host
（ナトリウムイオンホストとしてのハードカーボン電極の反応機構解析）

氏　　名　森川　裕介

## 1. General introduction

With the increasing social demand for a sustainable society, there is a strong need to transit from fossil fuels to renewable energy sources and from gasoline vehicles to electric vehicles. Since renewable energy sources (*e.g.*, solar, wind) do not produce electricity consistently, large-scale energy storage devices are required to store excess energy and stabilize power supply. Currently, lithium-ion batteries (LIBs) are mainly used as a power source for portable devices (*e.g.*, mobile phones, laptop computers), but it is strongly needed to expand to aforementioned large-scale applications in the future. However, the scarcity and uneven distribution of the constituent chemical resources hinder the large-scale use of LIBs. The sodium-ion battery (NIB), a classical analogue of LIBs, has attracted significant attention over the past decade as an alternative to LIBs because sodium is the second lightest alkali metal and its resources are widely available from the Earth's crust and the sea.

One of the most promising negative electrode materials for NIBs is non-graphitizable carbon, generally called “hard carbon”.[1,2] A schematic diagram of hard carbon is shown in **Fig. 1**. Graphitic domains are composed of curved and defective graphene sheets that loosely stacked with van der Waals forces. In addition, hard carbon has many small voids inside, called “nanopore”. It has been studied for almost 20 years as an anode material for NIBs, but sodium storage mechanism in hard carbon has not been fully understood due to its low crystallinity and diversity of microstructure.[4] In the present thesis, the correlation between the sodium storage behavior and the microstructure of

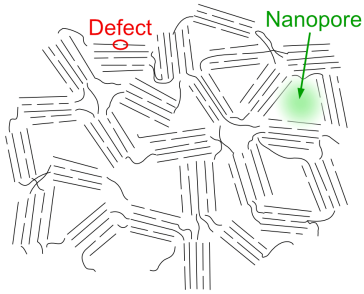


**Fig. 1** The schematic microstructure of hard carbon. Small graphitic domains are interconnected with each other in a disordered manner. The interstitial voids act as nanopores.[3]

hard carbon was systematically analyzed. Moreover, the author designed and optimized an electrolyte that dramatically improved the rate characteristics, which is a weak point of hard carbon, and investigated the reason for the improvement.

## 2. Synthesis of high-performance hard carbon for sodium-ion batteries

Prior to the reaction mechanism analysis, the author synthesized hard carbon with enhanced sodium storage capacity by optimizing raw materials and synthesis conditions. Moreover, to minimize the influence of the decomposition product of the electrolyte on the reaction mechanism analysis, the author aimed to improve the initial coulombic efficiency (ICE).

Hard carbon samples were synthesized by hydrothermal treatment of saccharides. It was found that hard carbon synthesized using a mixture of two kinds of monosaccharides has a large reversible capacity and high ICE. Hard carbon synthesized from a mixed aqueous solution of glucose: fructose = 1: 1 in molar ratio showed the maximum reversible capacity (283 mAh $g^{-1}$) and ICE (90.5%). X-ray diffraction (XRD) and small-angle X-ray scattering (SAXS) measurements revealed that the porosity of hard carbon greatly increased by mixing two types of sugars. After that, heat treatment was performed under Ar flow at temperatures (*T*) ranging from 1000 to 2000 °C to change the microstructure (*e.g.*, volume and size of nanopores, the distance between graphene–graphene layers, number of defects) and further improve the sodium storage properties. The prepared products are denoted HC-*T*. As a result, the HC-1400 had both the highest ICE (95.2%) and a relatively large reversible capacity (348 mAh $g^{-1}$) compared to the hard carbon reported in various papers in the past.

## 3. Sodium storage mechanism in hard carbon

The systematic sodium storage mechanism analysis was conducted using the hard carbons synthesized in Chapter 2.

Changes in the microstructure of hard carbon due to heat treatment were analyzed using XRD, SAXS, and Raman spectroscopy. The higher-temperature treatment caused a monotonic decrease of the interlayer distance and continuous increase of the average pore diameter because of progressive graphitization and rearrangement of graphene layers. The electrochemical measurements were conducted using half-cells to evaluate the Na storage properties. As the carbonization temperature was increased, a sloping region (>0.1 V) decreased and a plateau region (≤ 0.1 V) became dominant (**Fig. 2**). Based on these electrochemical properties, three hard carbons, HC-1000, HC-1400, and HC-1900, were selected for analysis to understand the overall Na storage mechanism in detail.

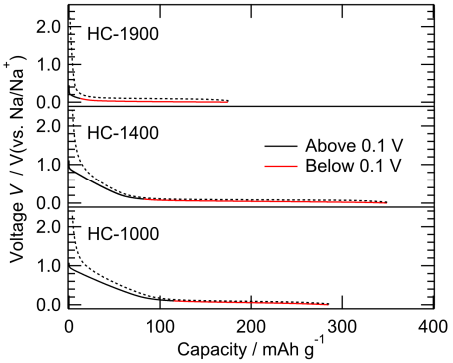


**Fig. 2** Galvanostatic charge–discharge curves of the hard carbons with varied carbonization temperatures at a current density of 20 mA $g^{-1}$.

For structural analysis of the sodiated hard carbons, *ex situ* wide-angle X-ray scattering (WAXS) and SAXS measurements were conducted. From WAXS analysis, it was confirmed that the reversible sodium

insertions to the interlayer space in the graphitic domains except for HC-1900. Notably, a new broad peak appeared at $q \approx 2.0$–$2.1$ Å$^{-1}$ in all the hard carbon samples at the plateau region and this peak became more pronounced upon further sodiation. After sodium metal nucleation, a sharp Bragg reflection from bulk sodium metal became detectable at $q = 2.07$ Å$^{-1}$, indicating that the deposition/dissolution reactions of bulk sodium metal do not occur at voltages above 0 V. From SAXS analysis, the reversible change in the scattering intensity from the nanopores was detected, demonstrating the nanopores act as reversible sodium storage sites. Furthermore, it was found that the number density of sodium atoms confined in the nanopores was comparable to that of bulk body-centered cubic (bcc) sodium.

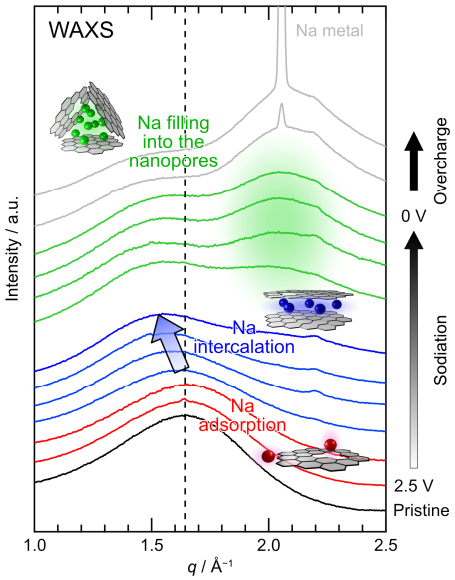


**Fig. 3** *Ex situ* WAXS patterns of hard carbon electrodes (HC-1000).

The nanopore filling process observed by SAXS is accompanied by a simultaneous emergence of another signal in the WAXS profile, as discussed above. Assuming that the origin of the new signal in the WAXS profile is the atomic correlation of sodium in the nanopores, the author performed WAXS simulations utilizing hypothetical atomic structures derived by DFT-based molecular dynamics (DFT-MD) simulations for various sizes of the Na assembly. Based on the calculation results, regardless of the diversity of sizes and structures, the scattering patterns have a characteristic broad peak at $q \approx 2.1$ Å$^{-1}$, which is assigned to the nearest neighbor Na–Na correlation.

## 4. Electrolyte design for hard carbon anode toward reversible and high-rate operation

A typical charge–discharge curve of hard carbon has a sloping region and a plateau region, and the latter constitute more than half of the overall capacity. Because of this low reaction potential, at which most organic compounds are reduced, selecting appropriate electrolyte components or functional binders is essential to achieve the reversible charge-discharge cycling of hard carbon electrodes. It is known that a stable solid electrolyte interphase (SEI) that improve cyclability of batteries can be formed by using fluorine-containing materials.[5,6] In chapter 4, sodium tetraphenylborate ($NaBPh_4$, structural formula is shown in **Fig. 4**a)/1,2-dimethoxyethane (DME) system that enables highly reversible Na metal plating/stripping[7] was applied to hard carbon anode.

Electrochemical measurements of hard carbon | Na metal half cells were performed using various electrolyte. The 0.5 M $NaBPh_4$/DME electrolyte exhibited the highest ICE of 95.0% with high capacity retention of 95.6% during 100 cycles, suggesting the minimized reductive decomposition of the electrolyte components for forming a stable SEI. Moreover, 0.5 M $NaBPh_4$/DME could retain a reversible capacity of over 200 mAh g$^{-1}$ even at a current density of 6000 mA g$^{-1}$ owing to low polarization, which is distinct from the almost zero capacity in conventional 1 M $NaPF_6$/EC:DEC (Fig. 4a).

The surface analysis of the cycled hard carbon electrodes via X-ray photoelectron spectroscopy shows that $NaBPh_4$ is not subjected to reductive decomposition during cycling and that the SEI is derived from ether solvent (Fig. 4b). With all things considered, the ether-derived SEI, though containing no fluorine component, is inherently stable and has low-resistivity, thus, the combination of ether solvent with reduction-tolerant $NaBPh_4$ salt is the most effective one to achieve highly reversible and high-rate cycling of hard carbon anodes.

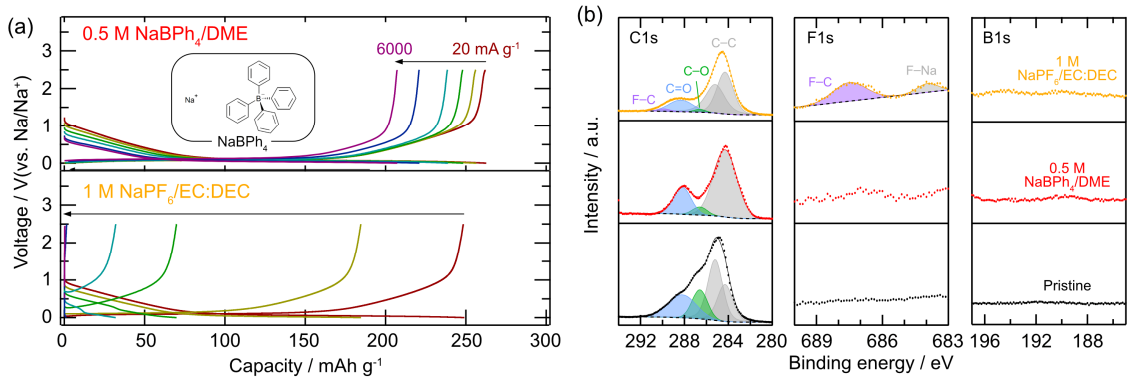


**Fig. 4** (a) Charge-discharge voltage profiles of hard carbon | Na metal half cells with various 0.5 M $NaBPh_4$ electrolytes as compared to a standard 1 M $NaPF_6$/EC:DEC at increasing current densities from 20 mA $g^{-1}$ to 6000 mA $g^{-1}$. (b) C1s, F1s, B1s XPS spectra of the hard carbon electrodes after three cycles in various electrolytes.

## 5. Conclusion

In summary, it was discovered that hard carbon with low ICE and large capacity can be synthesized by using a mixture of two types of monosaccharides in an appropriate ratio as a raw material. Subsequently, by *ex situ* analysis for synthesized hard carbon with continuously changed microstructure, the correlation between the microstructure of hard carbon and sodium storage behavior is clarified. The author has succeeded to detect a new broad peak in WAXS pattern as a signature of sodium insertion into the nanopores, and its origin was analyzed to be Na–Na correlation of Na assemblies in the nanopores using DFT-MD simulations for the first time. In addition, the author found the highly reversible and high-rate cycling of hard carbon electrodes in $NaBPh_4$/DME electrolyte, suggesting that fluorine species are not indispensable in stabilizing the hard carbon/electrolyte interface. Reduction stability of salt and solvent is considered to be the key to stable operation of negative electrode materials. The author believes this study makes meaningful contributions to give direction for designing hard carbon and new functional electrolytes for NIBs.

## References


[1] D. A. Stevens and J. R. Dahn, *J. Electrochem. Soc.*, **2000**, 147, 1271.

[2] S. Komaba *et al.*, *Adv. Funct. Mater.*, **2011**, 21, 3859.

[3] R. E. Franklin, *Acta Crystallogr.*, **1951**, 4, 253.

[4] D. Saurel *et al.*, *Adv. Energy Mater.*, **2018**, 8, 1703268.

[5] S. Komaba *et al.*, *ACS Appl. Mater. Interfaces*, **2011**, 3, 4165.

[6] R. Cao *et al.*, *Nano Energy*, **2016**, 30, 825.

[7] K. Doi *et al.*, *Angew. Chemie Int. Ed.*, **2019**, 58, 8024.